

# Rich State Observations Empower Reinforcement Learning to Surpass PID: A Drone Ball Balancing Study

Mingjiang Liu and Hailong Huang

**Abstract**—This paper addresses a drone ball-balancing task, in which a drone stabilizes a ball atop a movable beam through cable-based interaction. We propose a hierarchical control framework that decouples high-level balancing policy from low-level drone control, and train a reinforcement learning (RL) policy to handle the high-level decision-making. Simulation results show that the RL policy achieves superior performance compared to carefully tuned PID controllers within the same hierarchical structure. Through systematic comparative analysis, we demonstrate that RL’s advantage stems not from improved parameter tuning or inherent nonlinear mapping capabilities, but from its ability to effectively utilize richer state observations. These findings underscore the critical role of comprehensive state representation in learning-based systems and suggest that enhanced sensing could be instrumental in improving controller performance.

## I. INTRODUCTION

Aerial manipulation, which aims to endow aerial robots with the capability to physically interact with their surroundings [1], has attracted significant attention in recent years. The most common aerial manipulation systems employ unmanned aerial vehicles (UAVs) as floating bases and equip them with robotic arms or custom grippers. These configurations have been successfully applied to tasks such as millimeter-level peg-in-hole insertion [2], light bulb removal [3], and in-flight grasping [4]. Alternatively, manipulation can also be achieved through direct attachment or cable suspension, with cable-suspended payload transportation being a prominent example [5]–[7].

Despite these advances in aerial manipulation, significant challenges persist in real-world applications. Most existing systems are confined to direct physical contact, yet many practical scenarios require indirect manipulation, which involves interacting with objects via an intermediate tool or platform. For instance, during transportation, a robot might need to carry a box using a cable-suspended carrier. Here, the robot must manipulate the carrier rather than the box directly, while actively stabilizing it to prevent falling. Such forms of indirect manipulation introduce new challenges, especially in learning to control intermediary tools.

To explore the potential of indirect aerial manipulation, this paper studies a drone ball-balancing task (see Fig. 1), where a drone tethered to one beam end via a rope

The authors are with the Autonomous and Interactive Mobile Systems Group (AIMS), Department of Aeronautical and Aviation Engineering, The Hong Kong Polytechnic University, Hong Kong, China. Email: mingjiangaae.liu@connect.polyu.hk

This paper has been accepted for presentation at the Advancements in Aerial Physical Interaction Workshop of the IEEE/RSJ International Conference on Intelligent Robots and Systems (IROS), 2025. Comments and feedback are welcome.

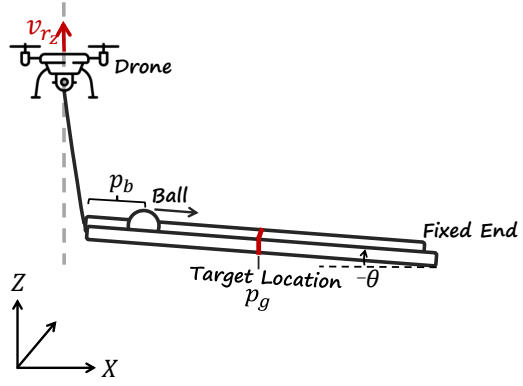


Fig. 1. Illustration of the drone ball-balancing task. The drone is tethered to one end of the beam while the opposite end is fixed. The goal of the drone is to guide the ball toward the target position by manipulating the beam.

and is required to manipulate a beam to position a ball at a target location. To solve this problem, we proposed a hierarchical control framework comprising: A high-level policy that generates velocity commands according to system state observations and a low-level velocity controller for precise reference tracking.

Motivated by recent advances in RL [8], [9], we formulated the drone ball-balancing task as a Markov Decision Process (MDP) and developed an RL-based high-level controller to address this problem. Specifically, we created a drone ball-balancing simulator using Isaac Lab [10]. To enable GPU-accelerated parallel training, we implemented a PyTorch-based low-level flight controller based on the SE(3) geometry controller [11]. The balancing policy was parameterized by a neural network and trained using the Robust Policy Optimization algorithm (RPO) [12].

Simulation experiments demonstrate that the RL-based policy exhibits excellent performance in the drone ball-balancing task. To further validate the superiority of the RL-based approach, we replaced the high-level RL agent with incremental PID controllers [13] within the same hierarchical framework. Empirical results reveal that PID controllers fail to stabilize the system, even when augmented with additional velocity constraints.

While numerous studies demonstrate RL’s superiority over classical control methods (e.g., PID and model predictive control (MPC)) in robotics [14]–[16], these findings remain largely empirical, lacking systematic analysis of the fundamental factors contributing to RL’s success or classical

methods' limitations. In contrast, a recent comparative study in autonomous drone racing [17] reveals that RL's advantage stems primarily from its ability to optimize more effective objectives. This insight provides a principled foundation for future method selection and advancement in similar robotic applications. Inspired by this work, we conducted systematic controlled experiments to investigate why RL outperforms PID control. Our results demonstrate that RL's superiority stems not from discovering superior control gains or employing nonlinear error mapping, but rather from its ability to leverage richer state observations for decision-making effectively.

## II. METHODOLOGY

### A. Hierarchical Framework

We proposed a two-layer control architecture as illustrated in Fig. 2 to solve the drone ball-balancing task.

The high-level controller generates strategic commands for beam inclination adjustment. Its operational workflow is: receiving real-time system state observations; computing an appropriate vertical velocity increment ( $\Delta v_{r_z}$ ) based on these observations; outputting this increment to be combined with the current drone velocity ( $v_{r_z}$ ), forming the reference velocity ( $v_{r_z} + \Delta v_{r_z}$ ). The high-level controller generates velocity increments rather than direct velocity commands to account for the drone's physical constraints. This approach ensures all commanded velocities remain within the drone's achievable acceleration limits, preventing the generation of kinematically infeasible reference velocities.

The low-level controller executes precise velocity tracking for the drone. It takes the reference velocity from the high-level controller and computes the corresponding rotor speeds for flight control. In this paper, we implemented a PyTorch-based controller based on the SE(3) geometry controller [11] to enable GPU-accelerated parallel training.

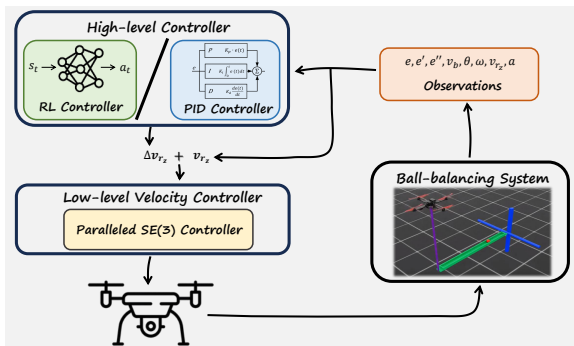


Fig. 2. Illustration of the proposed hierarchical control framework. The high-level controller generates optimal Z-axis velocity commands based on real-time system state observations, while the low-level controller ensures precise tracking of these commanded velocities.

### B. RL-based High-level Controller

A common practice in applying RL to robotics is to define the state, action, and reward function for the MDP. In the drone ball-balancing task, the drone's observations consist

of the state information of the ball-and-beam system and its own current state, represented as an 8-dimensional state vector:  $[e, e', e'', v_b, \theta, \omega, v_{r_z}, a]$ . Here,  $e$  denotes the position error between the ball's current position  $p_b$  and the goal position  $p_g$ ;  $e'$  is the first-order difference of the position error, calculated as  $e' = e_t - e_{t-1}$ ;  $e''$  is the second-order difference, computed as  $e'' = (e_t - e_{t-1}) - (e_{t-1} - e_{t-2})$ ;  $v_b$  represents the ball's velocity along the beam;  $\theta$  is the beam angle;  $\omega$  is the angular velocity of the beam; and  $a$  denotes the last action taken by the agent, which is the one-dimensional vertical velocity increment  $\Delta v_{r_z}$ . To formalize the control objective, we design a composite reward function as follows:

$$r = r_{\text{object}} + r_{\text{control}} + r_{\text{failure}} + r_{\text{goal}}, \quad (1)$$

where its components are mathematically defined as:

$$r_{\text{object}} = -k_1 e^2 - k_2 v_b^2, \quad (2a)$$

$$r_{\text{control}} = -k_3 v_{r_z}^2 - k_4 a^2, \quad (2b)$$

$$r_{\text{failure}} = \begin{cases} -k_5 & \text{if } (|\theta| > \theta_{\max}) \vee (|e| > e_{\max}) \\ 0 & \text{otherwise} \end{cases}, \quad (2c)$$

$$r_{\text{goal}} = \begin{cases} (c - \frac{c - c_{\min}}{e_{\text{goal}}} |e|) \times \exp(-k_6 |v_b|) & \text{if } |e| < e_{\text{goal}} \\ 0 & \text{otherwise} \end{cases}. \quad (2d)$$

Given the outstanding performance of RPO [12], it was selected to train the ball-balancing policy.

### C. PID-based High-level Controller

While PID control has demonstrated success in traditional ball-and-beam systems [18], its efficacy in the drone ball-balancing task remains unexplored. This work adopts an incremental PID formulation aligned with the design where the high-level controller outputs vertical velocity increments. The discrete-time implementation of this incremental PID controller follows:

$$a_{t_k} = K_p e'_{t_k} + \frac{K_p \Delta t}{T_i} e_{t_k} + \frac{K_p T_d}{\Delta t} e''_{t_k}, \quad (3)$$

where  $a_{t_k}$  denotes the drone's high-level commanded action at timestep  $t_k$ ,  $\Delta t$  represents the sampling time interval,  $K_p$  is the proportional gain,  $T_i$  and  $T_d$  are the integral and derivative time constants, respectively. Through extensive empirical tuning, we consistently observed system oscillations regardless of gain selection. However, these oscillations attenuated under vertical velocity constraints. This finding motivated our comparison with three distinct velocity constraint conditions: strict constraint (i.e.,  $|v_{r_z}| \leq 0.1\text{m/s}$ ), moderate constraint (i.e.,  $|v_{r_z}| \leq 0.3\text{m/s}$ ), and loose constraint (i.e.,  $|v_{r_z}| \leq 0.5\text{m/s}$ ). For each condition, we empirically determined optimal PID gains to enable a comprehensive performance comparison with the RL controller.

### III. EXPERIMENTS

#### A. Setups

To meet the data requirements for RL policy training, we developed a drone ball-balancing simulator using the Isaac Lab framework [10]. As shown in Fig. 2 (Ball-balancing System), one end of the beam is fixed at a constant altitude with a rotatable joint supporting the rotation of the beam, while the drone controls the tethered opposite end. The simulation uses Ascending Technologies' Hummingbird drone model.

For training the RL-based high-level policy, we designed both actor and critic networks as two-layer MLPs with 256 neurons per layer, where the actor's output layer employed a  $tanh$  activation function. Each training episode lasted up to 5 seconds, during which the drone needed to quickly position and stabilize the ball at the target. To mitigate instability issues during initial training phases, we implemented early termination when either the beam tilt exceeded  $\theta_{\max}$  or the ball detached from the beam. This mechanism significantly enhanced exploration efficiency. The control architecture operated with high-level policy updates at 60 Hz and low-level velocity tracking at 180 Hz to ensure stable and responsive control.

#### B. Results

1) *Evaluation Metrics*: The evaluation protocol runs 1000 test episodes, each lasting 10 seconds. For the RL-based controller, we report performance as means and standard deviations across five random seeds. This paper utilizes four evaluation metrics: success rate (SR), steady-state error (SE), convergence time (CONT), and climb time (CLIT). Specifically, SR calculates the percentage of episodes with absolute terminal position error below 0.01m; SE measures the absolute terminal position error; CONT tracks the time required for the ball to reach and stay within  $\pm 0.02$ m of the target; and CLIT captures the initial entry time into the target zone with position error 0.02m.

TABLE I

PERFORMANCE COMPARISON BETWEEN RL AND PID CONTROLLERS.

Controller	SR(%) <sup>†</sup>	SE(mm) <sup>‡</sup>	CONT(s) <sup>†</sup>	CLIT(s) <sup>‡</sup>
RL	$100 \pm 0$	$1.290 \pm 0.535$	$1.702 \pm 0.117$	$1.383 \pm 0.027$
PID with $ v_{r_z}  \leq 0.1$	100	1.919	2.623	2.622
PID with $ v_{r_z}  \leq 0.3$	61	9.548	3.508	1.107
PID with $ v_{r_z}  \leq 0.5$	14	30.275	9.977	0.952

2) *Performance*: The quantitative results, including the ball's position error and the drone's vertical velocity increment over time, are presented in Table I and Fig. 3, respectively. As shown in Table I, the RL-based controller achieves a 100% SR and outperforms all PID-based controllers in both SE and CONT. For the PID controllers with velocity constraints, the SR decreases as the constraints are relaxed, highlighting PID's limitations in this task. Interestingly, while the PID controller with  $|v_{r_z}| \leq 0.1$  achieves comparable performance to the RL-based method, its control actions (i.e., drone velocity increments  $\Delta v_{r_z}$ ) exhibit high-frequency oscillations (see Fig. 3 (b)). This indicates that the

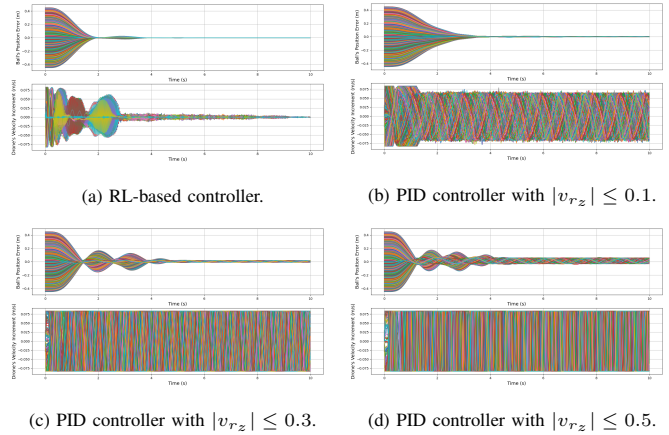


Fig. 3. Time evolution of the ball's position error and drone's vertical velocity increment for the drone ball-balancing task with  $p_g = 0.5$ . (a) demonstrates the RL-based controller's fast and stable performance, while (b)-(d) reveal oscillatory behavior in the PID controllers with velocity constraints, despite the position errors seeming to converge to the surrounding region of the target at (b) and (c).

system oscillates around the target position, a behavior that becomes more pronounced with looser velocity constraints (see Fig. 3 (c) and (d)).

### IV. WHY RL OUTPERFORMS PID

#### A. Hypotheses

We empirically propose three hypotheses to explain the performance differences between RL and PID control:

- *H1*: RL's gradient-based optimization enables discovery of more effective control parameters than PID's manual trial-and-error tuning.
- *H2*: RL's nonlinear policy mapping better handles the system's nonlinear dynamics compared to PID's linear control law.
- *H3*: RL's state representation, incorporating richer system information beyond position error, facilitates superior control decisions versus PID.

#### B. Experiment Design

Designing targeted experiments to validate each hypothesis presents significant methodological challenges. As an alternative approach, we evaluate RL performance using identical input features to the PID controller for direct comparison. Following Equation (3), we provide the RL actor with the same three-dimensional feedback  $(e, e', e'')$  used by the PID controllers. Simultaneously, we constrain the vertical velocity to make consistent comparison conditions with the PID controllers. However, to maintain learning efficiency, we implement a privileged critic architecture that retains access to the full 8-dimensional state space  $[e, e', e'', v_b, \theta, \omega, v_{r_z}, a]$  for state-action value estimation. To enhance training effectiveness, we developed a three-phase curriculum learning strategy:

- **Initial Phase**: Target neighborhood  $e_{\text{goal}} = 0.3$  with ball initialization outside this region.

- **Intermediate Phase:** Reduced target neighborhood ( $e_{\text{goal}} = 0.15$ ).
- **Final Phase:** Tight convergence requirement ( $e_{\text{goal}} = 0.05$ ).

This progressive approach ensures comprehensive coverage of the initial state space while gradually increasing task difficulty.

### C. Empirical Results

We trained RL policies using PID-equivalent inputs for the drone ball-balancing task with  $p_g = 0.5$  and evaluated their performance under identical conditions. As shown in Table II and Fig. 4, the RL controllers exhibit poorer performance compared to PID with velocity constraints, while also displaying characteristic oscillations around the target position.

This poor performance under identical inputs refutes hypotheses H1 (superior parameter optimization) and H2 (nonlinear mapping advantage), indicating that RL's performance benefits do not originate from these factors. However, when provided with full state feedback, RL demonstrates significantly improved performance. This strongly supports hypothesis H3, confirming that RL's advantage derives from its ability to leverage richer system information for more effective decision-making. This result highlights the potential for improving the controller's performance by deploying more sensors.

TABLE II  
PERFORMANCE OF RL USING PID-EQUIVALENT INPUTS WITH  
VELOCITY CONSTRAINT CONDITIONS.

Controller	SR(%) <sup>†</sup>	SE(mm) <sup>‡</sup>	CONT(s) <sup>†</sup>	CLIT(s) <sup>†</sup>
RL with $ v_{rz}  \leq 0.1$	$90.360 \pm 17.960$	$5.709 \pm 1.566$	$2.038 \pm 0.342$	$1.869 \pm 0.084$
RL with $ v_{rz}  \leq 0.3$	$36.040 \pm 14.702$	$20.447 \pm 11.361$	$9.697 \pm 0.321$	$1.709 \pm 0.060$
RL with $ v_{rz}  \leq 0.5$	$7.120 \pm 2.881$	$117.454 \pm 41.578$	$9.966 \pm 0.035$	$1.617 \pm 0.097$
RL without Constraint	$2.120 \pm 0.801$	$257.910 \pm 33.050$	$10.011 \pm 0.004$	$1.733 \pm 0.192$

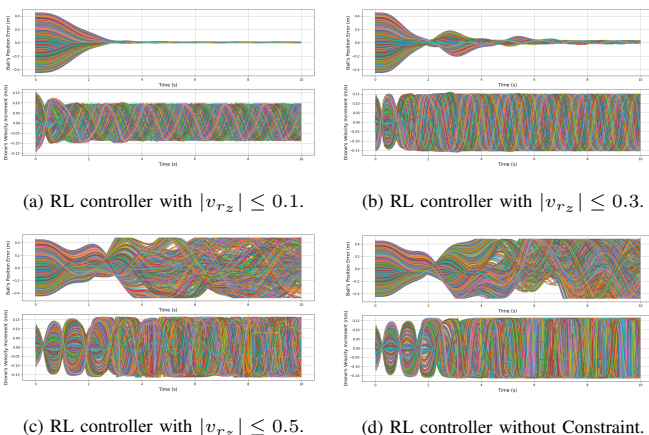


Fig. 4. Time evolution of the ball's position error and drone's vertical velocity increment for RL using PID-equivalent inputs in the drone ball-balancing task with  $p_g = 0.5$ .

### V. CONCLUSIONS

In this work, we investigate the potential of model-free RL for indirect aerial manipulation by proposing a hierarchical control framework with an RL-based high-level controller for a drone ball-balancing task. Simulated results demonstrate that the RL policy achieves better performance than PID control. Systematic analysis shows that this advantage stems primarily from RL's ability to exploit richer state information rather than from superior control parameter optimization or inherent nonlinear mapping capabilities. These findings underscore the critical role of comprehensive state representation in learning-based control systems and highlight the potential for improving controller performance through the deployment of additional sensors.0

### REFERENCES

- [1] A. Ollero, M. Tognon, A. Suarez, D. Lee, and A. Franchi, "Past, present, and future of aerial robotic manipulators," *IEEE Transactions on Robotics*, vol. 38, no. 1, pp. 626–645, 2021. [I](#)
- [2] M. Wang, Z. Chen, K. Guo, X. Yu, Y. Zhang, L. Guo, and W. Wang, "Millimeter-level pick and peg-in-hole task achieved by aerial manipulator," *IEEE Transactions on Robotics*, vol. 40, pp. 1242–1260, 2023. [I](#)
- [3] G. He, X. Guo, L. Tang, Y. Zhang, M. Mousaei, J. Xu, J. Geng, S. Scherer, and G. Shi, "Flying hand: End-effector-centric framework for versatile aerial manipulation teleoperation and policy learning," *arXiv preprint arXiv:2504.10334*, 2025. [I](#)
- [4] S. Ubellacker, A. Ray, J. M. Bern, J. Strader, and L. Carlone, "High-speed aerial grasping using a soft drone with onboard perception," *npj Robotics*, vol. 2, no. 1, p. 5, 2024. [I](#)
- [5] H. Wang, H. Li, B. Zhou, F. Gao, and S. Shen, "Impact-aware planning and control for aerial robots with suspended payloads," *IEEE Transactions on Robotics*, vol. 40, pp. 2478–2497, 2024. [I](#)
- [6] G. Li, X. Liu, and G. Loianno, "Human-aware physical human-robot collaborative transportation and manipulation with multiple aerial robots," *IEEE Transactions on Robotics*, vol. 41, pp. 762–781, 2025. [I](#)
- [7] Q. Quan, J. Xu, R. Liu, Y. Ding, J. Che, and K.-Y. Cai, "Self-organizing aerial swarm robotics for resilient load transportation: A table-mechanics-inspired approach," *arXiv preprint arXiv:2509.03563*, 2025. [I](#)
- [8] I. Radosavovic, T. Xiao, B. Zhang, T. Darrell, J. Malik, and K. Sreenath, "Real-world humanoid locomotion with reinforcement learning," *Science Robotics*, vol. 9, no. 89, p. eadi9579, 2024. [I](#)
- [9] D. Zhang, A. Loquercio, J. Tang, T.-H. Wang, J. Malik, and M. W. Mueller, "A learning-based quadcopter controller with extreme adaptation," *IEEE Transactions on Robotics*, vol. 41, pp. 3948–3964, 2025. [I](#)
- [10] M. Mittal, C. Yu, Q. Yu, J. Liu, N. Rudin, D. Hoeller, J. L. Yuan, R. Singh, Y. Guo, H. Mazhar, et al., "Orbit: A unified simulation framework for interactive robot learning environments," *IEEE Robotics and Automation Letters*, vol. 8, no. 6, pp. 3740–3747, 2023. [I](#), [III-A](#)
- [11] T. Lee, M. Leok, and N. H. McClamroch, "Geometric tracking control of a quadrotor uav on  $se(3)$ ," in *49th IEEE conference on decision and control (CDC)*. IEEE, 2010, pp. 5420–5425. [I](#), [II-A](#)
- [12] M. M. Rahman and Y. Xue, "Robust policy optimization in deep reinforcement learning," *arXiv preprint arXiv:2212.07536*, 2022. [I](#), [II-B](#)
- [13] A. Vissioli, *Practical PID control*. Springer Science & Business Media, 2006. [I](#)
- [14] J. Zheng, T. Zhang, C. Wang, M. Xiong, and G. Xie, "Learning for attitude holding of a robotic fish: An end-to-end approach with sim-to-real transfer," *IEEE Transactions on Robotics*, vol. 38, no. 2, pp. 1287–1303, 2021. [I](#)
- [15] A. S. Robbins, M. Ho, and M. Teodorescu, "Model-free dynamic control of robotic joints with integrated elastic ligaments," *Robotics and Autonomous Systems*, vol. 155, p. 104150, 2022. [I](#)
- [16] P. Zhai, T. Hou, X. Ji, Z. Dong, and L. Zhang, "Robust adaptive ensemble adversary reinforcement learning," *IEEE Robotics and Automation Letters*, vol. 7, no. 4, pp. 12562–12568, 2022. [I](#)

- [17] Y. Song, A. Romero, M. Müller, V. Koltun, and D. Scaramuzza, “Reaching the limit in autonomous racing: Optimal control versus reinforcement learning,” *Science Robotics*, vol. 8, no. 82, p. eadg1462, 2023. [I](#)
- [18] N. Muškinja and M. Rižnar, “Optimized pid position control of a nonlinear system based on correlating the velocity with position error,” *Mathematical Problems in Engineering*, vol. 2015, no. 1, p. 796057, 2015. [II-C](#)